Transmission laser welding of thermoplastics by using carbon nanotube web

M. Russello[1,*], G. Catalanotti[1,2,†], S.C. Hawkins[1,3], C.W. Chan[1], B.G. Falzon[1,4]

[1] *Advanced Composites Research Group (ACRG), School of Mechanical and Aerospace Engineering, Queen's University Belfast, Belfast BT9 5AH, UK*

[2] *Escola de Ciências e Tecnologia, Universidade de Évora, 7000-671 Évora, Portugal*

[3] *Department of Materials Science and Engineering, Monash University, Clayton 3800, Australia*

[4] *School of Engineering, RMIT University, Melbourne, 3001, Australia*

Abstract

Laser welding of transparent and semi-transparent thermoplastics using layers of carbon nanotube (CNT) web as absorbant is reported. Single lap shear specimens were manufactured placing the layers of CNT-web between two polyethylene terephthalate glycol-modified (PETG) sheets, that were successively irradiated with laser power at a wavelength of 1064nm. Optical analyses were performed to assess the transmittance of the joint under different configurations; for the single layer of CNT web a transmittance of 83%, in the visible range, was obtained after welding. Single-lap shear tests were performed and a shear strength of 23 MPa was obtained when using one layer of CNT-web. The investigated technology allows using a solid film as laser absorbing material, replacing conventional liquid or dye that need to be processed and applied on the surface before welding, thus speeding up the manufacturing process.

Keywords

Laser transmission welding; Thermoplastic; Carbon nanotube web; Transparent polymer; Solid absorbing material; Glycol-modified polyethylene terephthalate.

1 Introduction

Weld bonding of polymers, which entails the joining of components by melting the mating surfaces of plastic components, is nowadays indispensable in manufacturing, and the introduction of new techniques has extended the range of weldable structures and materials. Compared with traditional methods, the application of lasers to polymer welding offers several advantages and opportunities such as shorter processing time and excellent heat localization, with consistent quality and repeatability [1]. Moreover, the technique is contactless and generates minimal residual thermal stress in the part [1].

In Laser Transmission Welding (LTW), the laser beam passes through the first of the parts to be welded, which is transparent or semi-transparent to the laser wavelength, and then is absorbed and converted to heat at or very near the interface between the parts.

There are three main strategies to convert the laser beam energy into heat at the interface:

i) Lower Part Absorption: The upper part is transparent to the laser wavelength while the lower part is opaque, being compounded with appropriate absorbing additives (dyes or pigments). In this case, the laser beam passes through the upper part, to the surface of the lower part where it is converted into heat [1]–[3] (Fig.1a). The heat, then, is transmitted by conduction to the interface and upper part;

---

*Corresponding author. Email address: mrussello01@qub.ac.uk (Massimiliano Russello)

†Corresponding author. Email address: gcatalanotti@uevora.pt (Giuseppe Catalanotti)

ii) Interface Absorption: Both components are transparent but one or both surfaces at the interface bears an absorbing layer. This converts the laser energy into heat which is then delivered to the parts by thermal conduction (Fig. 1b);

iii) Bulk Absorption: If the parts are of a polymer that partially absorbs the radiation, a laser of the appropriate wavelength can be used, without additional dyes or absorbers, and the heat is generated in the bulk material with localization at the interface achieved with focussing [4][5] (Fig. 1c).

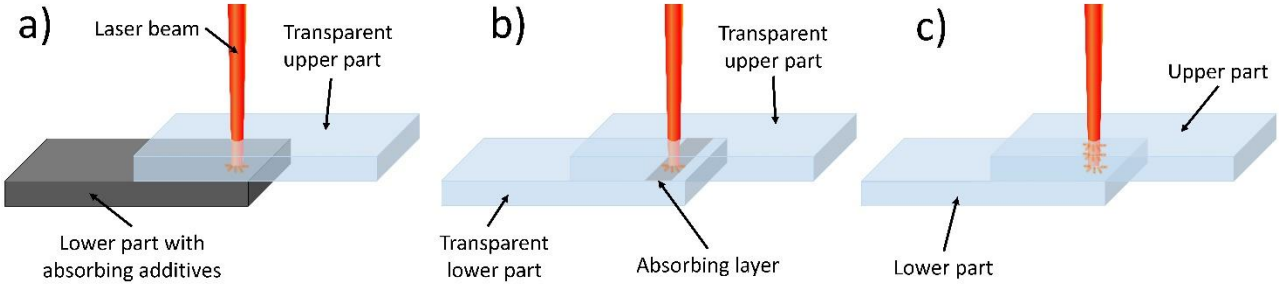

Figure 1 – Welding strategies where a) the lower part is compounded with absorbing additives, b) an absorbing layer is sandwiched between two transparent parts and c) the laser beam is directly absorbed by the parts at particular wavelengths.

In the latter case, for example, polycarbonate absorbs only around 10% of laser radiation in the range of 400 - 1500 nm but near 1700 nm absorbs 70% [4]. Nevertheless, the process is limited by the availability of suitable laser sources and lenses. Moreover, the use of different polymers with different optical properties and thickness makes the setup slow, complex, and inflexible.

Compounding the lower part to be joined with light-absorbing additives such as carbon black, which absorbs light almost equally well at wavelengths from 300 nm to 2500 nm [6], in polycarbonate [7] simplifies the joining method, however, the depth and efficiency of heating are very dependent on absorbent loading when used at reasonable levels (ie <1%). Other polymers, such as acrylic [1] with 0.2% and polypropylene with 0.1% and 0.3% [8] carbon black have also been studied however low loadings result in more heating occurring in the body of the absorbing part rather than at the interface, and any variation in loading uniformity results in uneven heating or poor heat transfer to the transparent part [8]. Higher loading of 2% in polypropylene produces effective heating at the interface [9],[10] and facilitates the modelling and study of process parameters such as laser energy and exposure time. Carbon nanotubes (CNT), which exhibit extremely efficient absorption of light at all wavelengths [11], can be used instead of carbon black as a dispersion in polymers for LTW.

For example, in ABS the carbon nanotube was used as an absorber with percentages ranging from 0.01 to 0.05 wt% and the absorbing components were produced by starting from a masterbatch with a high concentration of carbon nanotubes and subsequently, dissolution was performed in order to achieve the desired low concentration [12]. It was also shown that for low CNT concentration, the process window increases significantly while high concentration resulted in higher sensitivity to the variation of input power [12]. In polypropylene [13] carbon nanotube was used in conjunction with dispersed Fe_2O_3 and heating using an Nd:YAG laser at 532 nm with a concentration of 1 wt%. The use of carbon nanotube, compared to Fe_2O_3, resulted in higher shear strength (10 MPa against 4.5 MPa). Carbon nanotubes were also used to weld polyethylene sheets in concentrations ranging from 0.1 to 10 wt% [14]. The experimental results

highlighted that the laser light absorbing polymeric sheet, filled with carbon nanotubes, must have a low filler amount (about 0.1 wt%), just enough to smelt the two parts avoiding defect formation.

Whereas carbon black and CNT loaded polymers remain opaque black after welding, dispersed transparent strongly absorbing fluorescent dyes such as those based on squaraine [2] have also been demonstrated. Although initially highly coloured, the dyes can be permanently bleached with heat or UV light after welding. This novel approach presents some technical difficulties as the dye starts to degrade at a temperature of 150 ℃ so the dye dispersion process must be carefully controlled to avoid excessive temperatures. The dyes themselves are complex and expensive to produce and require lasers of particular wavelengths e.g. 623-670 nm [1]. Commercially available Lumogen IR ® products based on the more thermally stable and nearly colourless but strongly IR absorbing rylene [15] molecular structure are now available. These products require a laser at around 800 nm but have limited suitability for PP and PE polymers.

The use of dispersed dyes and pigments for LTW means that two different polymer compositions – the absorbing material and the transmitting material – must be prepared, significantly increasing processing costs. The dye itself, which may be very expensive compared with the polymer, must nevertheless be dispersed uniformly throughout the absorbing batch at a relatively high concentration to achieve efficient heating near the interface even though only the absorber material nearest that interface is used for welding. An alternative approach is to apply an absorber at the interface only, which ensures that heating is concentrated and symmetrically distributed. A series of almost colourless IR absorbing dyes was developed around 2007 by Clearweld ® which however require a very uniform application (eg by spraying) of solutions in organic solvents prior to joining, and again requires a laser of the appropriate wavelength (from 940 nm to 1100 nm depending on the product). The products however do not appear to be available any longer.

To address the shortcomings of the existing Laser Transmission Welding techniques, we now demonstrate the use of CNT as an absorber but with interface application rather than dispersion. The stability, polymer compatibility and exceptional absorption characteristics of CNT over an extreme range of wavelengths, coupled with direct interface application make this the most attractive approach for LTW of thermoplastics. The uniform and extremely thin CNT layer necessary to achieve effective bonding without excessively darkening clear polymers is obtained with directly drawn CNT-web.

CNT-web has recently been employed in thermoplastic welding technologies [16] as an electrical susceptor that converts, by Joule effect, the electrical power into heat. However used now as an optical absorber, the web has a constant, uniform and reliable wavelength absorption over a wide spectral range and can be laid directly on the parts to weld. The web, directly drawn from a specially grown CNT forest[17], can have any planar dimension but is only around 50 nm thick, with an areal mass of around 20 mg/m^2. Each web layer is characterized by primary transparency of around 72%, which increases to around 83% after welding. In this research, the manufacturing process, the optical parameters and preliminary mechanical performance are investigated.

2 Materials and methods

2.1 CNT-web production and preparation

Directly drawable CNT forests, with an average CNT length of 300 μm, and an average diameter of 10 nm, were synthesized by chemical vapour deposition (CVD) following a procedure reported in [17]. The CNT-web is generated

by drawing the nanotubes from the front face of the CNT forest held on the silicon growth substrate, hence the CNT are highly aligned in the direction of draw (Fig. 2a). A single layer of CNT-web has an as-drawn thickness of about 20 μm which can be densified to around 50 nm. The web may potentially have indefinite length and width, however in this work, we use a web with a width of 30 mm.

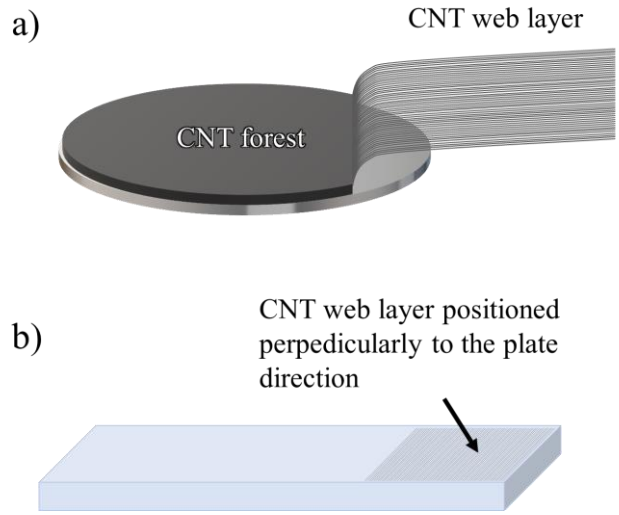

Figure 2 – a) Drawing of carbon nanotube web from CNT forest and b) PETG plate bearing the web.

Sheets of glycol-modified polyethylene terephthalate (PETG) with a thickness of 3 mm, were cut into rectangular plates of dimension 100 mm x 25 mm and then, after cleaning with *iso*-propyl alcohol to remove grease and dust, the CNT-web was directly laid on the surface of the plates at one end. The web was oriented perpendicularly to the longitudinal dimension and covered an area of 30 mm × 25 mm (Fig. 2b). The web can be used as initially laid but is easily disturbed. It is very effectively stabilised and secured on the polymer surface by 'solvent densification' whereby a solvent (eg *i*-PrOH), that does not dissolve the polymer, is applied as a fine spray or, as in this case, flowed across the plate dropwise from a disposable pipette and allowed to dry.

2.2 Welding process

In the present work, a fibre laser (MLS-4030, Micro Laser Systems, Netherlands) operating, by happenstance, at a wavelength of 1064 nm with a programmable X-Y stage was used as a heating source. All the experiments were run at a defocus distance of 23 mm to provide an appropriate heating profile over a reasonable area. The laser spot has a diameter $w = 800$ μm at this defocus distance.

Transmission laser welding variables can be identified by two types of parameters, namely absorber parameters, such as the intrinsic absorbance of, and the number of layers and orientation of the CNT-web; and process parameters, such as irradiation power, translation speed (feed rate), spot size, and pressure applied to the parts during irradiation. Although the study of all these variables would require a complex and broad design of experiments (DOE), the aim of the present work is to identify a reasonable parameter set to establish a preliminary prioritisation of variables and a demonstration of mechanical performance and optical properties. Samples used for tests were laser welded at the irradiation power $W = 1.83$ W, and pressure $p = 4$ MPa. Feed rates were varied as a proxy for energy input and heating rate with $v = 1$, 2.5, and 5 mm/s.

Two polymer plates, one bearing the densified CNT-web and one (the pristine plate) without, were overlapped by 30 mm length to form a single-lap shear test sample with the CNT in between. They were held between steel blocks and pressure applied using a double effect pneumatic cylinder (Festo ADVC-80-25-I-P) at air pressure of 6 bar to apply a load of 3 kN over the 25 mm x 30 mm contact area (resulting pressure 4 MPa). The plates, (Fig. 3b), were laser treated through a slot machined in the upper block (Fig. 3c). Given that the slot, with dimension 3 mm x 30 mm, was small compared to the overlapped area of the polymer plates, the pressure was assumed to be uniform over the contacting surface.

The laser system was programmed to generate weld lines oriented longitudinally to the sample direction (i.e. perpendicular to the CNT-web). Welded areas, *A*, of nominally 3 mm x 25 mm were generated across the sample by raster scanning parallel laser lines of nominal line width 800 μm and 800 μm apart (Fig. 3d). The scan length was 5 mm to give a 1 mm overlap with the clamping block at the start and end of each scan to eliminate any timing or dwell variability (Fig. 3d).

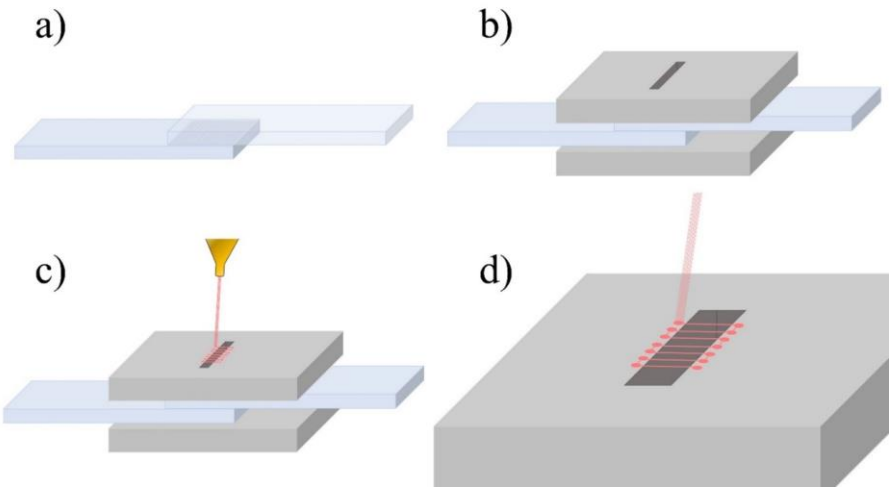

Figure 3 – a) Overlap of two polymer specimens prior to welding, b) clamping of the overlapped specimens between the plate of the compression tool, c) laser welding process through a machined slot to form 1 welding area and d) a detail of the laser path.

For each sample, five welding areas (Fig. 4), 3 mm apart, were generated one beside each other to create a pattern of welded and unwelded areas.

The melt pool produced by the laser will be wider than the beam diameter by an amount dependent upon the power transferred and the thermal conductivity of the web and polymer. Effective welding is achieved when contiguous weld pools substantially merge.

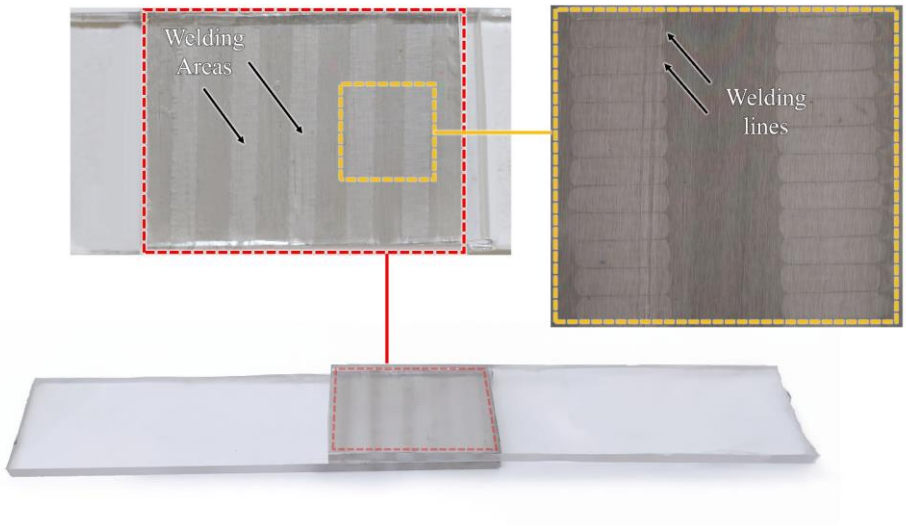

Figure 4 – Welded sample with 5 weld areas 3 mm apart (lighter zones) and in the detail the single weld lines each 800 um wide.

2.3 Optical characterization through a photographic method

2.3.1 Methodology

Additional optical information, obtained through a calibrated photographic method, was used for the quantitative assessment of the overall sample area (as distinct from the small area encompassed by a spectrophotometer) for uniformity and transmittance.

A camera (Canon EOS 80D mounting the Canon EF 100mm f/2.8L Macro IS USM lens), positioned perpendicularly to a flat light source (LCD display) and at a distance of 350 mm, was set to manual and camera parameters (shutter speed, iso, aperture and focus distance) were maintained constant throughout the whole process to ensure the proper comparison between the images. Lens stabilization was set to off and focus to manual.

Photographs of the light source (white LCD display) only (control image), and then of the test samples, positioned onto the display, were obtained in a dark room in RAW format (.CR2). RAW images, as distinct from other formats, are typically stored in linear-light values, where, after a noise correction (dark current correction), the captured light intensity from a light source is directly proportional to the value attributed to the pixels in the image (e.g. halving the emitted light intensity causes the pixel value to be halved). Test samples, positioned above the display, absorb part of the light which in turn hit the camera sensor producing an average pixel value lower than the one produced by the light source only. Thus, the transparency of an object can be computed as the ratio between the average pixel value of the test sample image and the control image (light source).

2.3.2 Dark current correction

Every camera sensor produces a certain amount of dark current, which accumulates in the pixels during an exposure. The dark current is produced by heat and the main problem is that it accumulates at a different rate in every pixel and it shifts up the pixel value of a certain amount causing the loss of proportionality with the incident light intensity. Fortunately, this effect can be easily removed by subtracting a dark frame.

A dark frame is a photograph taken under the same conditions (shutter speed, iso, aperture), but with no light striking the pixel array (e.g. putting the lens cap). The dark frame can be subtracted from the light frame to remove the fixed pattern from the image. For most sensors, this produces a striking improvement in the image.

ImageJ software with the DCRAW plugin, which enables to import RAW images at 16-bit linearly, was employed to subtract the dark frame from each test image.

ImageJ creates a corrected resulting 16-bit image, separated in its three colour channels, red, green, and blue. This image was then used for the assessment of pixel values and transparency.

2.3.3 The linearity of the method

The linearity between captured light intensity and pixel value was demonstrated as follows.

First, the light source (Fig. 5a) was photographed with no samples on it, and then, in sequence, with one, two, three and four overlapped PETG plates (Fig. 5b,c,d,e) (shutter speed equal to 1/10 sec, iso 100, aperture of f/2.8 and focus distance of 350 mm).

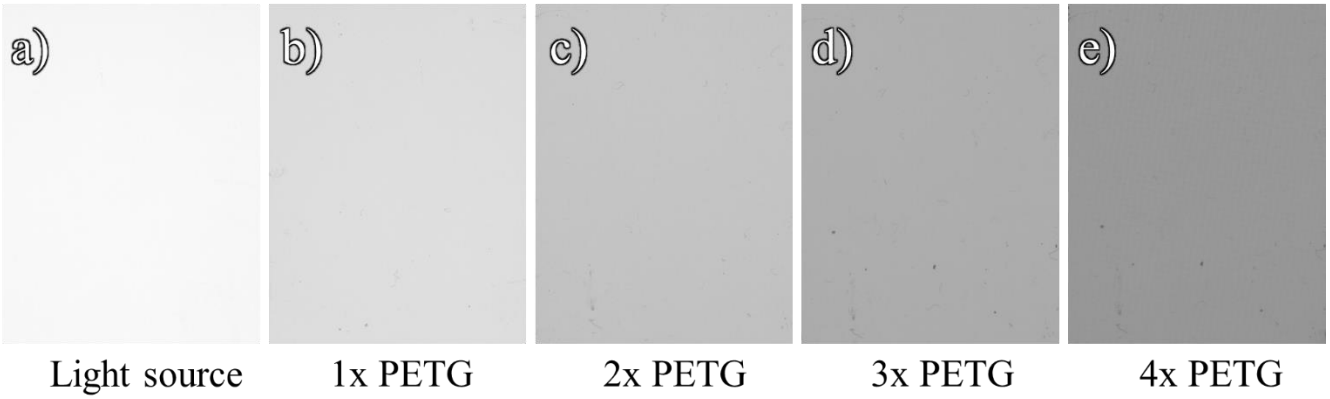

Figure 5 - Photographs of a) the light source and above samples.

Each added polymer plate, having the same light-absorbing properties (same thickness and material), would absorb the same amount of light (e.g. two plates will have double absorbance compared to one plate) and, for each picture, the pixel value would proportionally decrease. All images were dark current corrected and then, ImageJ software was used to evaluate the average pixel value of each image as follows.

For each sample image, i, and each colour channel, c, the average pixel values $\overline{\varphi}_{i_c}$, evaluated over a rectangular selection of 1500x2200 px in the middle of each image, were measured and used for evaluation of transmittance.

The transmittance, T_{i_c}, was calculated as:

$$T_{i_c} = \frac{\overline{\varphi}_{i_c}}{\overline{\varphi}_{d_c}} \times 100 \quad (1)$$

Where, $\overline{\varphi}_{d_c}$, is the average pixel value evaluated for the light source only (control image).

Finally, the absorbance, for each image and each channel, was computed as:

$$a_{i_c} = 2 - log_{10} T_{i_c} \quad (2)$$

Table 1 reports all data and calculations for transmittance and absorbance.

Table 1 – Measurements and calculation of average pixel value, transmittance and absorbance of the light source and PETG samples.

#	Average pixel value, $\overline{\varphi}_{ic}$			Transmittance %, T_{ic}			Absorbance data, a_{ic}		
	red	green	blue	red	green	Blue	Red	green	blue
Light source	12456	14507	18643	100.0	100.0	100.0	0.0000	0.0000	0.0000
1x PETG	10991	12741	16317	88.2	87.8	87.5	0.0543	0.0564	0.0579
2x PETG	9738	11247	14379	78.2	77.5	77.1	0.1069	0.1105	0.1128
3x PETG	8599	9904	12430	69.0	68.3	66.7	0.1609	0.1658	0.1760
4x PETG	7717	8855	11306	62.0	61.0	60.6	0.2079	0.2144	0.2172

As can be seen in table 1, the absorbance, of for example the red channel, almost proportionally increases with the number of PETG plates, whereby, one plate has an absorbance of 0.0543, while two, three or four overlapped plates have an absorbance which is near double, triple, and quadruple respectively. For each channel, Fig. 6, shows a near-perfect linear fit between the measured absorbance and the expected absorbance calculated considering a perfectly proportional behaviour.

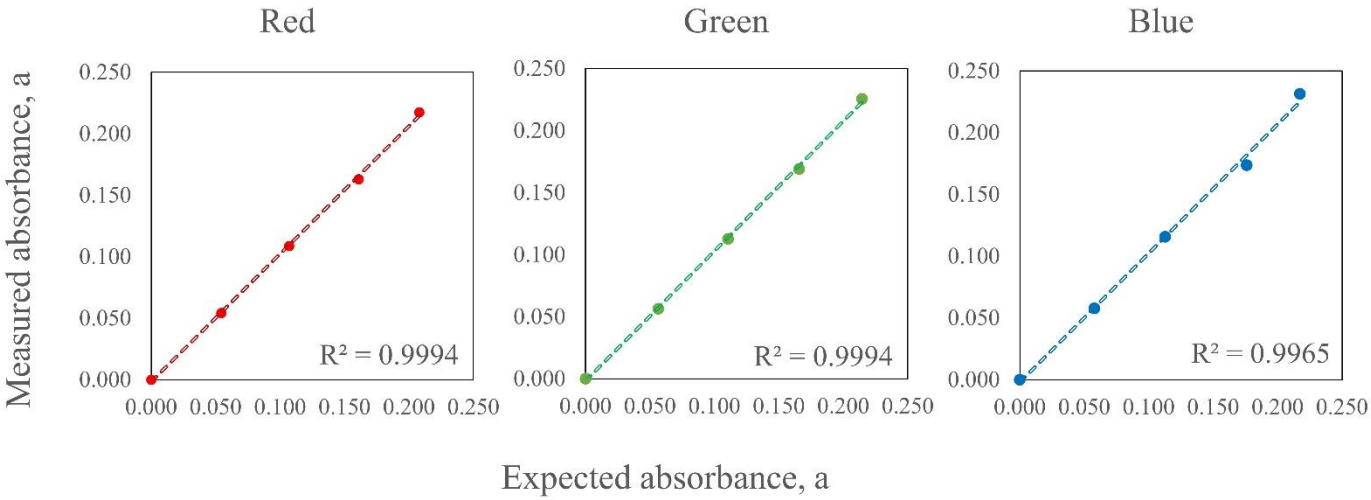

Figure 6 – Measured absorbance for each sample plotted against the expected linear absorbance.

Finally, the absolute value of transparency measured with an Agilent Cary 60 UV-VIS spectrophotometer was compared to the photographic method's results. Fig. 7 shows that the average transmittance in the range of 300 to 1100 nm, which include the visible spectrum, is around 90%, which, in turn, correspond to the transmittance value measured for a single PETG plate using the photographic method.

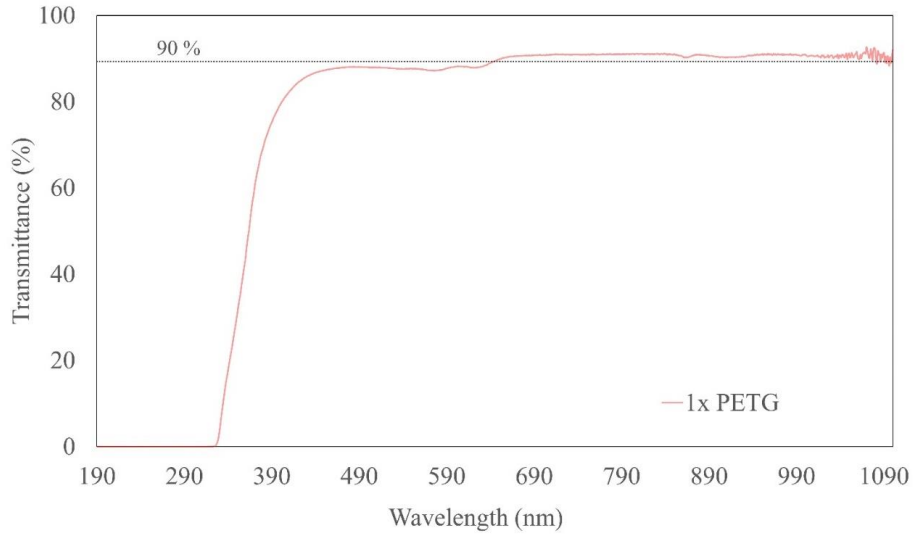

Figure 7 – Transmittance values, measured through UV-VIS spectrophotometer, of one single plate of PETG.

The same methodology was used to examine the transmittance and absorbance of carbon nanotube web layers. When compared to spectrometer results, this methodology allows for the investigation of a larger area of a sample and the elimination of errors caused by the small encompassed area provided by the spectrophotometer.

2.3.4 Transparency of the Carbon nanotube web layers under different light condition

Carbon nanotube webs, because of their structural nature, are characterized by the polarizing effect. A polarizing material, consisting of a polarization axis, lets light waves parallel to this axis pass through while blocking other waves of other polarization.

The ideal polarizing material, when hit by a random or circular polarized light source of intensityI_0, will transmit only one of the two linear components of light, reducing the initial unpolarized intensity by half, hence:

$$I = \frac{I_0}{2} \tag{3}$$

When the light source is already linearly polarized (the light lay on a single propagation plane) and of intensity I_0, the intensity Itransmitted through an ideal polarizer can be described by Malus' law,

$$I = I_0 cos^2\theta \tag{4}$$

where θ is the angle between the incident polarization light and the polarization axis. When the propagation plane of the linear polarized light is parallel to the polarization axis ($\theta = 0°$) the intensity is $I = I_0$, when it is perpendicular ($\theta = 90°$) the intensity is equal to zero.

Optical properties of carbon nanotube web layers were measured under two different light sources:

i) Circularly polarized display (CPD).

ii) Linearly polarized display (LPD).

For each light source, photographs of the following were captured:

i) Light source image (control image),

ii) two overlapped PETG plates without CNT web layers (2xPETG)

iii) welded samples (welding feed rate $v = 5$ mm/s), comprised of two PETG plates, containing one (1CNTL), or two CNT web layers (2CNTL).

Test samples, containing the single (Fig. 8c and d) or double (Fig. 8e and f) CNT web layer, were positioned on the display with the carbon nanotube web layers oriented longitudinally (Fig. 8c and e) and perpendicularly (Fig. 8d and f) to the display direction to detect information at different angles.

The use of circularly polarized light should show no difference in the transmitted or absorbed light when samples are placed at 0 or 90°, however, since light source can suffer of small errors in the generation of a perfect circularly polarized light, measurements were exectuted at both angles and the average value was used for comparison.

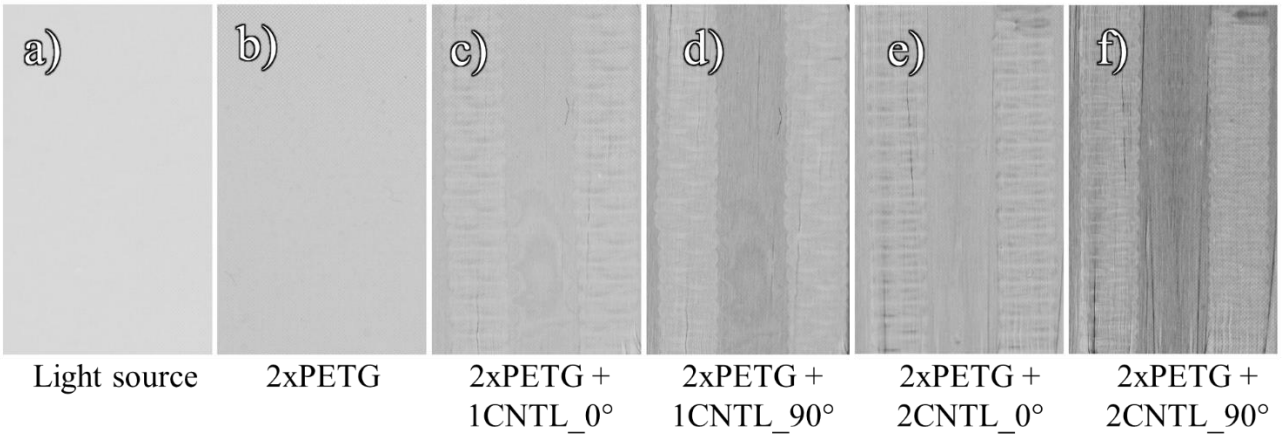

Figure 8 – Photographic comparison between the a) light source b) two overlapped polymer plates, two welded samples positioned at c) 0° and d) at 90° containing 1 layer CNT-web and c) two welded samples positioned at e) 0° and f) at 90° containing 2-layers CNT-web.

Using ImageJ software, images were all black frame corrected and finally the average pixel value $\overline{\varphi}_{i_c}$, evaluated for each image i and each colour channel c, was measured over a rectangular selection of 1500x2200 px for the control image (display) and the 2xPETG image, and over a rectangular selection of 1500x1100 px for welded and unwelded areas of welded samples containing one and two web layers and positioned at 0 and 90° (Tab. 2).

Table 2- Designation of sample and configuration for the measurement of pixel value using ImageJ software.

Designation, #	Angle, °	Area of interest,	Selection size, px
Light source	0	/	1500×2200
2xPETG	0	/	1500×2200
2xPETG+1CNTL_0°_u	0	unwelded	1500×1100
2xPETG+1CNTL_0°_w	0	welded	1500×1100
2xPETG+1CNTL_90°_u	90	unwelded	1500×1100
2xPETG+1CNTL_90°_w	90	welded	1500×1100
2xPETG+2CNTL_0°_u	0	unwelded	1500×1100
2xPETG+2CNTL_0°_w	0	welded	1500×1100
2xPETG+2CNTL_90°_u	90	unwelded	1500×1100
2xPETG+2CNTL_90°_w	90	welded	1500×1100

Finally, the transmittance and absorbance read:

$$T_{i_c} = \frac{\overline{\varphi}_{i_c}}{\overline{\varphi}_{d_c}} \times 100 \quad (1)$$

$$a_{i_c} = 2 - log_{10} T_{i_c} \quad (2)$$

where, $\overline{\varphi}_{d_c}$, is the average pixel value evaluated for the light source (control image). For each configuration the average values across each channel of transmittance and absorbance, $\overline{T_i}$ and $\overline{a}_i$, were computed as reported in Tables 3 and 4.

Table 3 – Average pixel value, transmittance and absorbance data for sample positioned above a circularly polarized light source.

#	Average pixel value, $\overline{\varphi}_{i_c}$			Transmittance %, T_{i_c}				Absorbance data, a_{i_c}			
	red	green	blue	red	green	blue	Avg. $\overline{T_i}$	red	green	blue	Avg. $\overline{a}_i$
Light source (CPD)	12456	14507	18643	100.0	100.0	100.0	100.0	0.000	0.000	0.000	0.000
2x PETG	9738	11247	14379	78.2	77.5	77.1	77.6	0.107	0.111	0.113	0.110
2xPETG+1CNTL_0°_u	7726	8323	10195	62.0	57.4	54.7	58.0	0.207	0.241	0.262	0.237
2xPETG+1CNTL_0°_w	8198	9406	11726	65.8	64.8	62.9	64.5	0.182	0.188	0.201	0.190
2xPETG+1CNTL_90°_u	7066	7910	10005	56.7	54.5	53.7	55.0	0.246	0.263	0.270	0.260
2xPETG+1CNTL_90°_w	8186	9321	11766	65.7	64.3	63.1	64.4	0.182	0.192	0.200	0.191
2xPETG+2CNTL_0°_u	5822	6686	7878	46.7	46.1	42.3	45.0	0.330	0.336	0.374	0.347
2xPETG+2CNTL_0°_w	6672	7607	9244	53.6	52.4	49.6	51.9	0.271	0.280	0.305	0.285
2xPETG+2CNTL_90°_u	5328	5826	7346	42.8	40.2	39.4	40.8	0.369	0.396	0.404	0.390
2xPETG+2CNTL_90°_w	6451	7222	9044	51.8	49.8	48.5	50.0	0.286	0.303	0.314	0.301

Table 4 – Average pixel value, transmittance and absorbance data for sample positioned above a linearly polarized light source.

#	Average pixel value, $\overline{\varphi}_{i_c}$			Transmittance %, T_{i_c}				Absorbance data, a_{i_c}			
	red	green	blue	red	green	blue	Avg. $\overline{T_i}$	red	green	blue	Avg. $\overline{a}_i$
Light source (LPD)	9726	10766	12661	100.0	100.0	100.0	100.0	0.000	0.000	0.000	0.000
2x PETG	7636	8412	9910	78.5	78.1	78.3	78.3	0.105	0.107	0.106	0.106
2xPETG+1CNTL_0°_u	6392	6936	7967	65.7	64.4	62.9	64.4	0.182	0.191	0.201	0.191
2xPETG+1CNTL_0°_w	6690	7248	8313	68.8	67.3	65.7	67.3	0.163	0.172	0.183	0.172
2xPETG+1CNTL_90°_u	4896	5280	6029	50.3	49.0	47.6	49.0	0.298	0.309	0.322	0.310
2xPETG+1CNTL_90°_w	6169	6739	7833	63.4	62.6	61.9	62.6	0.198	0.203	0.209	0.203
2xPETG+2CNTL_0°_u	5439	5820	6573	55.9	54.1	51.9	54.0	0.252	0.267	0.285	0.268
2xPETG+2CNTL_0°_w	5642	6043	6840	58.0	56.1	54.0	56.1	0.237	0.251	0.267	0.252
2xPETG+2CNTL_90°_u	3197	3384	3774	32.9	31.4	29.8	31.4	0.483	0.503	0.526	0.504
2xPETG+2CNTL_90°_w	4474	4842	5583	46.0	45.0	44.1	45.0	0.337	0.347	0.356	0.347

The absorbance of carbon the CNT-web only, $\overline{a}_{CNT}$, for each configuration, was then computed as the difference between the average absorbance of the welded samples $\overline{a}_{sample}$(having the absorption contribution of 2 PETG plus the CNT web layers) and the average absorption of the 2xPETG plates, $\overline{a}_{2PETG}$:

$$\overline{a}_{CNT} = \overline{a}_{sample} - \overline{a}_{2PETG} \tag{5}$$

2.4 Sample preparation for mechanical tests

Lap shear tensile tests on welded samples were conducted using a Lloyd universal testing machine, equipped with a 5 kN load cell with a measurement accuracy of +/-0.1% full scale throughout the entire range of the sensor's rated capacity, at a cross-head speed of 1 mm/min. The shear strength σ_w was measured as:

$$\sigma_w = P/A \tag{6}$$

where P is the maximum load and A is the welded area.

For the mechanical test, a welded area, A, of nominally 3 mm x 6.4 mm in the middle of the overlap zone was created by raster scanning only 8 parallel laser lines (nominal line width 800 µm) at 800 µm intervals (Fig. 9). The small size of the welded area compared with the overlap zone prevents the fracture of the substrates (as confirmed by preliminary experiments) and promotes a cohesive type of fracture of the bond thus allowing proper shear characterization. The melt pool produced by the laser will be wider than the beam diameter by an amount dependent upon the power transferred and the conductivity of the web and polymer. Effective welding is achieved when contiguous weld pools substantially merge. Thus, the effective overall weld area will be slightly larger than 3 mm x 6.4 mm.

An optical microscope was used to inspect the width and the uniformity of the welded specimens.

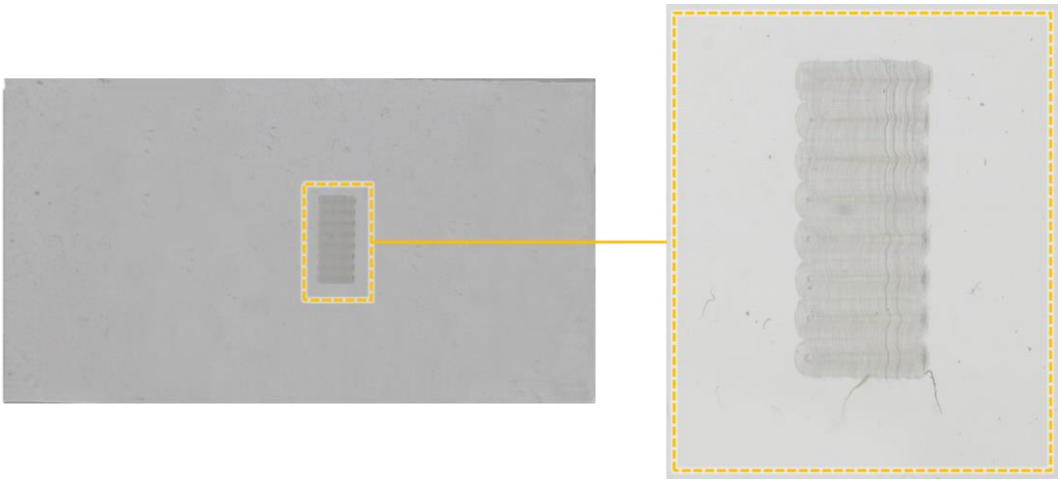

Figure 9 – Detail of the welded area for samples prepared for single lap join test.

3 Results and discussion

3.1 Optical Characterisation

Fig. 10 shows the results in terms of transmittance or absorbance for the layers of CNT-web under circularly polarized light.

The single CNT-web layer has a transmittance of 73% over a consistent wavelength range investigated, from 400 nm to 700 nm. This means that 27% of incident energy is absorbed and converted to heat by the 50 nm thick web placed at the interface while the rest of the energy is absorbed by the bulk polymer or transmitted through. The single layer, after welding, experiences an increase in transparency to 83%.

The 2-layers CNT-web presents an average transmittance of 55% (its average absorbance is double compared to the absorbance of the 1-layer CNT-web) while after welding it rises to 66%. As can be seen also in the absorbance chart of Fig. 10, the CNT-web is a "classic" absorber where for example 2 × absorbance of 1 layer = absorbance of two layers.

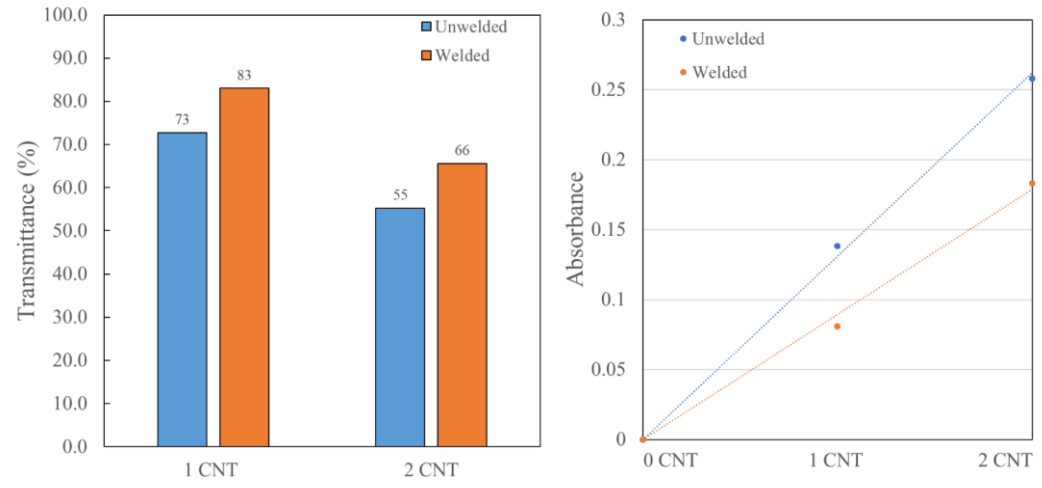

Figure 10 – Charts presenting the values of transmittance and absorbance for isolated CNT web layers positioned above a circularly polarized light source.

Under the linear polarized light (Fig. 11), the single CNT-web layer reveals a considerable difference between the specimens positioned at 0 and 90 degrees. Samples aligned with the direction of polarization have a transmittance of 82% (absorption = 0.085) while it decreases to 63% (absorption= 0.204) at 90°. This means that when the CNT layer is positioned perpendicular to a linearly polarised light, the single layer absorbs more than double the electromagnetic radiation (18% against 37%). It is also worth noting that, when compared to samples subjected to circular polarised light or random polarised light, which, as previously stated, absorbed 27% of the light, using a linearly polarised light and positioning the samples perpendicular to it increased the absorption to 37%. This would not only make the process more energy efficient, but would also eliminate the need for two layers, allowing for a high level of sample transparency.

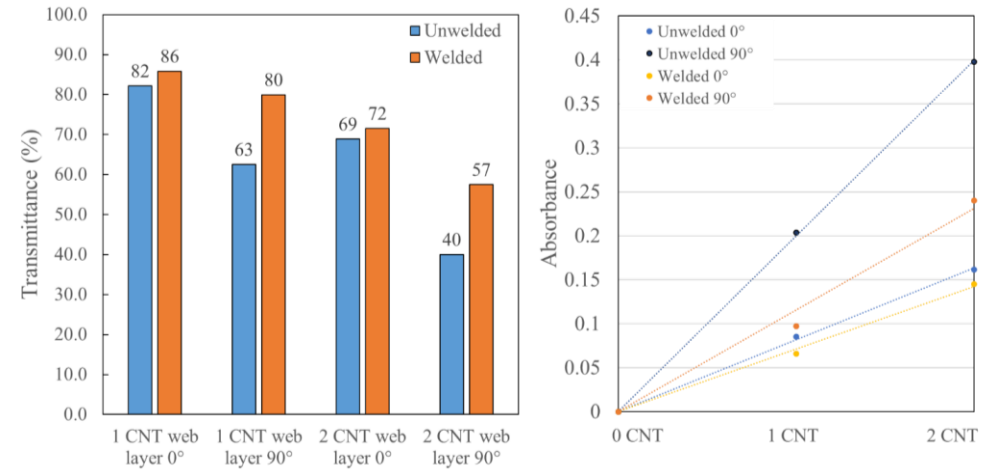

Figure 11 – Chart and data presenting the values of transmittance and absorbance for isolated CNT web layers positioned above a linearly polarized light source.

Finally, the 2-layers CNT-web has a transmittance of 69% at 0° (double absorption compared to the single layer at the same angle) while its transmittance decreases to only 40% at 90 degrees.
Also in this case and as expected, the absorbance of each sample follows a near-linear behaviour according to the Beer-Lambert law.

Measurements were also investigated using a UV-VIS spectrophotometer (Fig. 12). However, compared to the photographic method, slightly different results were found for the single and double layer of unwelded CNT web which result equal to 64 and 47% respectively (against 73 and 55% according to the photographic method). This difference is normally correlated to the known misreading of the detector of the spectrophotometer when an incident light beam passes through a polarizing material. Nonetheless, this chart shows that the transmittance (absorbance) for the single or double layer of CNT-web is almost flat through the analysed range from 330 to 1100nm. This means that previous results, investigated through the photographic method, are to be extended to the same range. This suggests also that different laser systems, working at a different wavelength, can be utilized on the same material having the same heating effect.

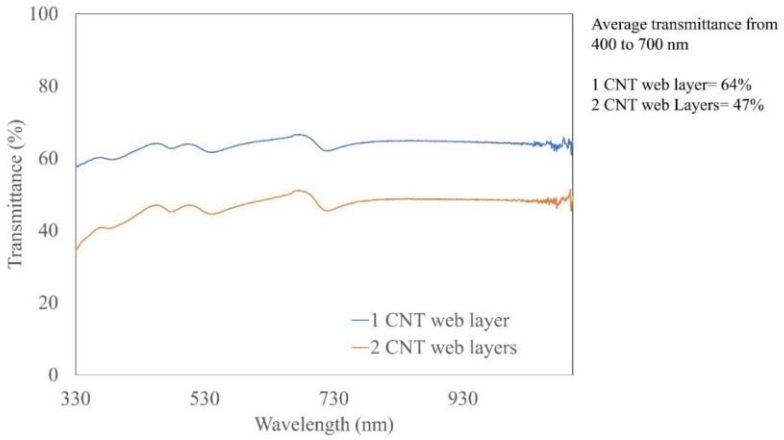

Figure 12 – Transmittance values, measured through UV-VIS spectrophotometer, of the single and double layer of CNT web

3.2 Effect of the energy density

Different laser parameters, such as specific power W_s, speed v and pressure p were initially investigated to understand the effect on weld efficiency and quality. The energy density, E, (energy per unit of area delivered to the weld) will depend upon power, W, speed, v, and spot size, w, and is defined as:

$$E = \frac{W}{vw} \tag{7}$$

An additional parameter is the absorbance of the susceptor, which will govern the amount of heat produced. Two layers of CNT web will absorb almost twice the energy compared to a single web. This effect is demonstrated with welding results for one and two layers of CNT web using the same weld parameters ($W = 1.83$ W, $p = 4$ MPa, $v = 5$ mm/s, raster spacing 800 μm). Fig. 13 shows the microscope observation (top view of welded interface) in correspondence with the ending part of the welded lines for samples containing one (Fig. 13a) and two (Fig. 13b) layers of CNT web. The higher energy absorption that characterized the two CNT web layers configuration produces a wider melt pool and hence a wider welding width, which causes the merging of contiguous weld lines. Multiple and perhaps crossed layers of CNT webs might be utilised where laser power is limited or where opacity, polarization or other factors are to be considered. For current weld quality and efficiency studies, a single layer of CNT web was used.

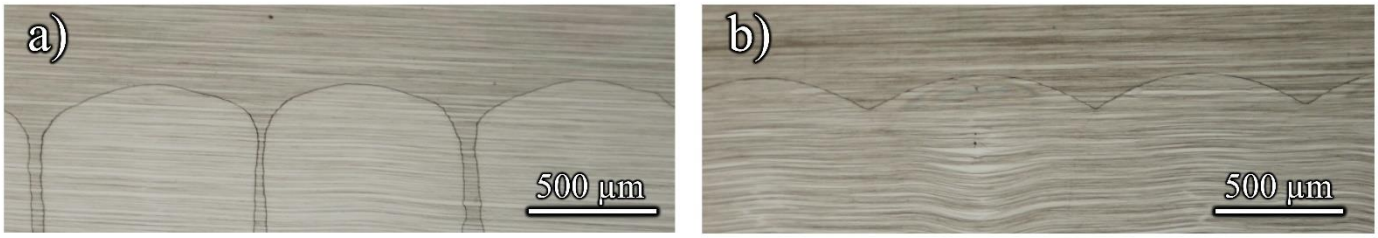

Figure 13 – Welding lines side by side for samples bearing a) 1-layer CNT-web and b) 2-layers CNT-web

Thus, for a given susceptor absorbance, spot size, w, the same energy density at the weld site, E, can be achieved either using 'high' laser power, W, and high welding speed, v, or 'low' power and low welding speed (the terms 'high' and 'low' being relative). However as heat is generated at the CNT web, it is also spreading into the surrounding web and being conducted into the bulk polymer to produce a heat affected zone (HAZ) the extent of which will depend on the duration and rate of heating. Heat dissipation means that laser power below an absolute limit will fail to melt the

polymer even when stationary, and welding can only proceed where the scan rate is slow enough to enable melting to occur. However, at low powers and speeds, the process becomes less and less energy efficient since most of the power is dissipated into the polymer far from the welding joint whilst also creating a deep HAZ. In contrast, when high power (e.g $W \approx 2$ W) plus high speed ($v = 5$mm/s for an energy density $E = 0.44$ J/mm^2) are adopted, and for the same weld pressure (e.g. $p = 4$ MPa), the heating, with less time for heat dissipation, is concentrated at the interface and welding is successful (Fig. 14a). However, if the power is too high then even with a higher speed to produce the same energy density, (e.g. $W \approx 8$ W, $v = 20$ mm/s), an excessive temperature increase occurs which degrades the polymer and the carbon nanotubes (Fig. 14b).

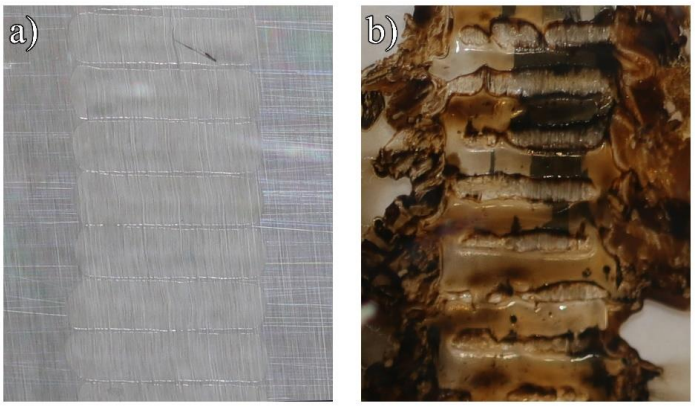

Figure 14 – a) Welding lines of a) samples welded with $W \approx 2$ W, $v = 5$ mm/s and b) samples welded with $W \approx 8$ W, $v = 20$ mm/s.

3.3 Mechanical performance

The single-lap shear strength was investigated for specimens containing 1 layer of CNT-web welded with a constant power $W = 1.83$ W at different scan rates (hence different energy density) and under a pressure $p = 4$MPa. At the fastest scan rate of 5 mm/s, the shear strength is only around 13 MPa, (Fig. 15). This calculation assumes that the total weld area is 3 × 6.4 mm. At a welding speed of 2.5 mm/s, the weld lines are merged and shear strength increased to around 19 MPa. However, a further speed reduction (and hence increase in power density) to 1 mm/s gives a further increase in strength to around 23 MPa.

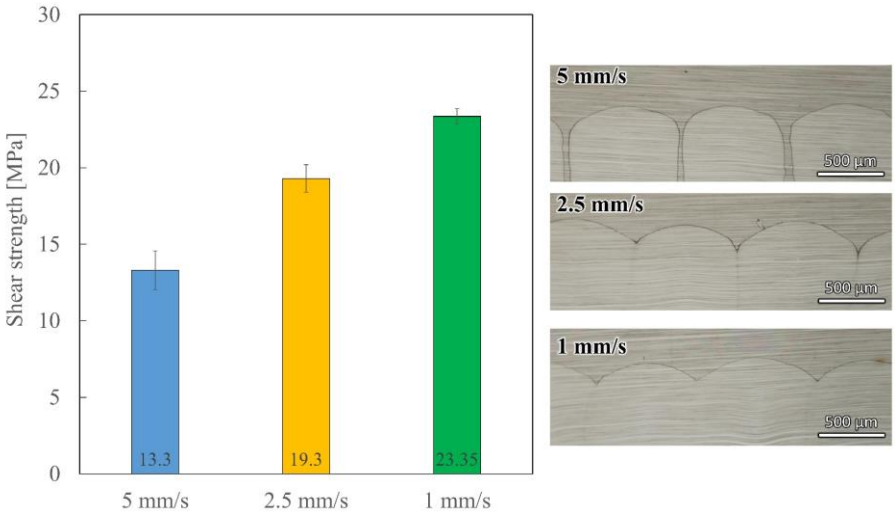

Figure 15 – Average and standard deviation of shear strength for specimens welded at 5, 2.5 and 1 mm/s respectively and observed welding lines for the same samples.

The two surfaces to be joined are separated by a CNT-web layer of at least 50 nm thickness, and the welding process is localised heating where the majority of the surrounding material remains unheated and hence solid. The only mechanism by which the polymer on either side of the join can come into contact and mix is if it melts and swells above the local surface. In the absence of pressure, such swelling may simply push the surfaces apart and bonding would not occur. The pressure applied externally must be sufficient to resist the internal pressure and force the expanding and molten but still highly viscous polymer pool to penetrate the CNT web and intermix with the polymer on the opposite face. The pressure also accommodates any slight mismatches in the surfaces to be joined and ensures uniform conduction from the CNT-web to the bulk material on both sides, and the effect of insufficient pressure is striking. For example, specimens welded with the same welding parameters as before (W =1.83 W, v =5 mm/s) but with the applied pressure reduced by only 50% from p =4 MPa to p =2 MPa had shear strength reduced from 13 MPa to only 1 MPa.

It should be noted that, although the strength obtained here can be used for material screening and qualification of the manufacturing process, this does not represent in any way a material parameter since it depends on the geometry of the welded region.

4 Conclusion

An innovative transmission laser welding method for transparent and semi-transparent thermoplastic, using CNT-web layers as an absorber, has been demonstrated. The web can be produced continually and can be easily scaled. The optical analysis, under circularly polarized light, has demonstrated that 1-layer CNT-web has a transmittance of 73%. This means that almost 30% of incident light is transformed into heat during welding. However, after welding, the transmittance of the web exhibits an increase of 15%, from 73 to 83% making the final product even more transparent.

The optical study has demonstrated that each CNT web layer has the same absorbance, thus, if for example a higher absorbance is required, a stack of multiple CNT web layers can be created to multiply the effect.

Also, optical analysis under linearly polarized light has shown that the single layer of CNT web, when positioned perpendicularly to the direction of light polarization (e.g. linearly polarized laser beam), transmit only 63% of energy. This means that around 37% of the energy is transformed into heat. Instead, when positioned parallel to the polarized light, it will only absorb 18% letting the left 82% pass through.

Different process parameters were investigated for preliminary understanding and single-lap shear tests have demonstrated a maximum shear strength of 23 MPa for samples welded using 1-layer CNT-web.

The demonstrated welding technology offers the potential of speeding up traditional welding processes, removing limitations on the range of laser source usable, and maintaining an excellent appearance for transparent components.

Finally, it is envisaged that the investigated technology would not be limited to thermoplastics, and could be used for other classes of transparent or semitransparent materials.

Acknowledgements

This work was supported by the project SPaRK which has received funding from the European Union's Horizon 2020 research and innovation programme under the Marie Sklodowska-Curie grant [grant agreement No 754507].

References

[1] B. Acherjee, D. Misra, D. Bose, and K. Venkadeshwaran, "Prediction of weld strength and seam width for laser transmission welding of thermoplastic using response surface methodology," *Opt. Laser Technol.*, vol. 41, no. 8, pp. 956–967, 2009.

[2] H. Ø. Bak, B. E. Nielsen, A. Jeppesen, T. Brock-Nannestad, C. B. O. Nielsen, and M. Pittelkow, "Laser welding of polymers using unsymmetrical squaraine dyes," *J. Polym. Sci. Part A Polym. Chem.*, vol. 56, no. 19, pp. 2245–2254, Oct. 2018.

[3] H. Potente, J. Korte, and F. Becker, "Laser Transmission Welding of Thermoplastics: Analysis of the Heating Phase," *J. Reinf. Plast. Compos.*, vol. 18, no. 10, pp. 914–920, Jul. 1999.

[4] V. Mamuschkin, A. Olowinsky, S. W. Britten, and C. Engelmann, "Investigations on laser transmission welding of absorber-free thermoplastics," *Laser-based Micro- Nanoprocessing VIII*, vol. 8968, p. 896815, 2014.

[5] J. De Pelsmaeker *et al.*, "Clear to clear laser welding for joining thermoplastic polymers: A comparative study based on physicochemical characterization," *J. Mater. Process. Technol.*, vol. 255, no. December 2017, pp. 808–815, May 2018.

[6] D. Han, Z. Meng, D. Wu, C. Zhang, and H. Zhu, "Thermal properties of carbon black aqueous nanofluids for solar absorption," *Nanoscale Res. Lett.*, vol. 6, no. 1, p. 457, 2011.

[7] B. Acherjee, A. S. Kuar, S. Mitra, and D. Misra, "Effect of carbon black on temperature field and weld profile during laser transmission welding of polymers: A FEM study," *Opt. Laser Technol.*, vol. 44, no. 3, pp. 514–521, 2012.

[8] F. Becker and H. Potente, "A step towards understanding the heating phase of laser transmission welding in polymers," *Polym. Eng. Sci.*, vol. 42, no. 2, pp. 365–374, 2002.

[9] I. Hadriche, E. Ghorbel, N. Masmoudi, and G. Casalino, "Investigation on the effects of laser power and scanning speed on polypropylene diode transmission welds," *Int. J. Adv. Manuf. Technol.*, vol. 50, no. 1–4, pp. 217–226, 2010.

[10] E. Ghorbel, G. Casalino, and S. Abed, "Laser diode transmission welding of polypropylene: Geometrical and microstructure characterisation of weld," *Mater. Des.*, vol. 30, no. 7, pp. 2745–2751, 2009.

[11] J. Lehman, C. Yung, N. Tomlin, D. Conklin, and M. Stephens, "Carbon Nanotube-Based Black Coatings," *arXiv*, vol. 011103, no. December 2017, Sep. 2017.

[12] E. Rodríguez-Vidal, I. Quintana, and C. Gadea, "Laser transmission welding of ABS: Effect of CNTs concentration and process parameters on material integrity and weld formation," *Opt. Laser Technol.*, vol. 57, pp. 194–201, Apr. 2014.

[13] L. Torrisi, F. Caridi, A. M. Visco, and N. Campo, "Polyethylene welding by pulsed visible laser irradiation," *Appl. Surf. Sci.*, vol. 257, no. 7, pp. 2567–2575, 2011.

[14] A. M. Visco, N. Campo, L. Torrisi, and F. Caridi, "Effect of carbon nanotube amount on polyethylene welding process induced by laser source," *Appl. Phys. A*, vol. 103, no. 2, pp. 439–445, May 2011.

[15] Z. Yuan *et al.*, "Processable Rylene Diimide Dyes up to 4 nm in Length: Synthesis and STM Visualization,"

Chem. - A Eur. J., vol. 19, no. 36, pp. 11842–11846, Sep. 2013.

[16] M. Russello, G. Catalanotti, S. C. Hawkins, and B. G. Falzon, "Welding of thermoplastics by means of carbon-nanotube web," *Compos. Commun.*, vol. 17, pp. 56–60, Feb. 2020.

[17] S. C. Hawkins, J. M. Poole, and C. P. Huynh, "Catalyst Distribution and Carbon Nanotube Morphology in Multilayer Forests by Mixed CVD Processes."